Icarus 276 (2016) 163–169

Contents lists available at ScienceDirect

Icarus

journal homepage: www.elsevier.com/locate/icarus

Transport and electrodynamical coupling of nano-grains ejected from the Saturnian rings and their possible ionospheric signatures

W.-H. Ip[a,b,c,*], C.-M. Liu[d], K.-C. Pan[b]

[a] Institute of Astronomy, National Central University, Taiwan
[b] Institute of Space Science, National Central University, Taiwan
[c] Space Science Institute, Macau University of Science and Technology, Macau, China
[d] Department of Aerospace Engineering, Tamkang University, Taiwan

ARTICLE INFO

Article history:
Received 30 October 2015
Revised 31 March 2016
Accepted 5 April 2016
Available online 28 April 2016

Keywords:
Planets and satellites
Rings—planets and satellites
Atmospheres—planets and satellites
Magnetic fields

ABSTRACT

Besides oxygen-bearing neutral gas and ions, the Saturnian rings could be a source of small dust particles of nano-meter size range. Electrostatic charging effect by photoemission and/or electron impact could lead to ejection of the nano-grains out of the ring plane by electromagnetic force. The orbital motion of low-velocity charged dust generated by mutual collision of the ring particles has been considered in previous work (Liu and Ip, [2014], ApJ, 786, 34.). In the present parametric study, the dust component produced by meteoroid bombardment is modelled. Depending on the plasma environment in the vicinity of the rings and the condition of electrostatic charging at the ring plane, the transport mechanism could be modulated by the sunlit angle on the ring plane. It is found that, besides negatively charged dust, positively charged nano-grains could play a potentially important role in transporting water into the mid-latitude region of the Saturnian ionosphere in both hemispheres. Positively charged tiny grains could be injected into low-inclination escape trajectories away from Saturn. In addition to the modification (depletion) of Saturn's ionospheric electron content, this gravito-electromagnetic mass transport effect might modulate the water loading mechanism associated with the quasi-periodic formation of the Great White Spots and the planet-circling storms in the northern hemisphere. The present sets of simulations also suggest that the correlation the H_3+ emission pattern with the ring opacity distribution could be a consequence of a source mechanism in addition to quenching by the so-called "ring rain" effect.

1. Introduction

The Saturnian ring system provides a natural laboratory to study the formation of small bodies in the dust disk of the primordial solar nebula (Charnoz et al., 2010; Ohtsuki, 1993; Hyodo and Ohtsuki, 2014) as demonstrated by the Cassini observations of the "propeller" features (Tiscareno et al. 2013a) and outgrowth at the outer edge of the A ring (Murray et al. 2014). The interaction of the planetary magnetosphere and the ring particle might also be an important channel for mass exchange between the rings and the ionosphere as demonstrated by the formation of the sharp boundary between the B and C ring (Northrop and Hill, 1982, 1983; Ip, 1983a, 1984a; Northrop & Connerney, 1987). In addition, the injection of water and oxygen ions and charged grains of nano-meter size could play a significant role in depleting the ionospheric electron content (Connerney and Waite, 1984; Moses & Bass, 2000, Moore et al. 2006; Tseng et al., 2010). Because of the combined effect of the planetary gravitational force and Lorentz force constrained by the axially symmetric dipole field with center-offset by 0.04 R_S in the northern direction (Connerney et al., 1982), the precipitation pattern is asymmetrical. That is, ions or charged nano-grains with charge-to-mass ratio (q/m) smaller than 10^{-5} e/amu (or electronic charge to atomic mass unit), if launched initially in Keplerian motion at the ring plane with radial distance inside the orbital instability limit of 1.53 R_S, will move along the magnetic field line until hitting the planetary surface at mid-latitute in the southern hemisphere (Bouhram et al., 2006; Luhmann et al., 2006; Tseng et al., 2010; Liu and Ip, 2014). This theoretical prediction is inconsistent from the radio occultation measurements that a significant electron density bite-out occurs near the equatorial region (Moore and Mendillo, 2007). Even though a significant fraction (~ 17%) of the water-group neutrals in the neutral gas cloud of Enceladus origin will impact on the rings (Jurac and Richardson, 2005, 2007), it is noted that they would not be directly injected into the equatorial region of the

* Corresponding author at: Institute of Astronomy, National Central University, Taiwan. Tel.: +886 3 4026018; fax: +886 4262304.
E-mail address: wingip@astro.ncu.edu.tw (W.-H. Ip).

http://dx.doi.org/10.1016/j.icarus.2016.04.004
0019-1035/

Saturnian atmosphere. Instead, most of the water molecules will recondense on the surfaces of the ring particles in the outer A ring (Jurac and Richarcdson, 2007) and be recycled into the ring atmosphere. The final impact sites on Saturn's surface would still be guided by the magnetic field as described earlier.

This might be indicative of a new pathway for equatorial injection of positively charged icy nano-grains as discussed in Liu and Ip (2014). In this scenario, a population of small grains is constantly generated by mutual low-velocity ($\sim$ a few m s^{-1}) collisions among the ring particles. The main source region is distributed between the inner edge of the B ring and the synchronous orbit at 1.87 R_s. Because of the absorption effect of the ring particles, the ambient plasma density is very low thus resulting in predominantly positive charge of the dust grains (Ip, 1984b).

Because the ring plane is subject to hypervelocity impact by interplanetary meteoroids (Morfill et al., 1983, Tiscareno et al. 2013b), a component of high velocity ejecta should exist. Nano-grains could be created in the impact process or generated by recondensation of the expanding hot vapor cloud. What would be their corresponding trajectories and how might they interact with the planetary ionosphere are topics of importance to the unique investigation of the Cassini Proximal Mission in 2016–2017. The present work is organized as follows. Section 2 will describe the model and calculations. The results will be presented in Section 3. A summary and discussion will be given in Section 4.

2. Trajectory calculation

The impact velocity (v_i) of interplanetary meteoroids of micron-size at the Saturnian rings varies according to their orbital distribution in the outer solar system and the locations of ring plane crossing (Ip, 1995). With a range of v_i between 25 and 40 km/s, the expectation is that a volume of impact vapor of high temperature will be created. For example, from laboratory experiments of hyper-velocity impact of submicron particles on metallic surfaces, it was found that the temperature of the expanding vapor could be of the order of 2500–5000 K (Eichhorn, 1976; Collette et al, 2013). In the impact plume, smoke particles of nano-meter size could form during its adiabatic expansion. Because of the icy composition, the temperature of the vapor plumes of the Saturnian ring particles from micro-meteoritic bombardment might be lower. Taking the vapor temperature to be 2500 K, the outflow speed of these recondensed grains can be estimated to be on the order of 1.5 km/s.

Because the particle motion in the direction perpendicular to the ring plane will be least subject to collisional scattering and absorption, we can first consider the nano-grains of impact origin to have an initial velocity in the vertical direction. It is further assumed that the grains will be electrostatically charged to a charge-to-mass ratio in the range between 10^{-5} and 10^{-7} e/amu, either positively or negatively.

The subsequent trajectory of the charged dust grain is described by the equation of motion:

$$\frac{d\mathbf{v}}{dt} = \frac{q}{m}(\mathbf{E} + \mathbf{V} \times \mathbf{B}) - \frac{GM}{r^2}\hat{\mathbf{r}}$$

where G ($=6.7 \times 10^{-11}$ $m^3 s^{-2} kg^{-1}$) is the gravitational constant, M is the mass of Saturn, m is the mass of the dust grain, q is the charge, r is the radial distance from the planetary center, V is the grain velocity, the corotational electric E= $-V_c$ xB, with B as the planetary magnetic field and V_c as the corotation velocity. We further assume that the density of the dust grain is $\rho = 1000$ kg m^{-3}. From $q/m = 1.683 \times 10^{-9}$ $\phi_v/a_\mu{}^2$ [e/amu] with ϕ_v in volts and the grain radius a_μ in microns, we find $q/m = 10^{-5}$ (ϕ_v/6 V) [e/amu] if $a_\mu = 0.013$ (i.e., $a = 13$ nm).

3. Results

Fig. 1 is a summary of the particle trajectories for negatively charged grains with q/m between 10^{-5} and 10^{-7} e/amu, emitted upward with an initial vertical velocity of $v_z = 1.5$ km s^{-1}. The magnetic field model used in the present calculations has its dipole moment aligned with Saturn's spin axis and the dipole center has an offset of 0.04 R_s (Saturn radius) in the upward direction. The magnetic field strength at the magnetic midplane is $B_o = 0.21$ G. The panels from (a) to (c) describe the motion of the charged grains. The trajectories in the ϱ-z projection plane where ϱ is the perpendicular distance to the central axis and those projected onto the x–y plane of the rotating coordinate system of Saturn are given in the upper and lower panels, respectively. Because of the vertical shift of the magnetic moment, for launching site inside the Northrop-Hill instability limit of 1.53 R_s, the nano-grains would generally reverse its direction after the initial upward movement (see Fig. 1a). Once crossing the equatorial plane the particle with $q/m = 10^{-5}$ e/amu will continue to move along the magnetic field line until hitting the planetary surface. For those emitted outside the Northrop-Hill instability limit, they will be confined to bounce motion in the vicinity of the mid-plane. As is well known, the B-ring with its inner edge at 1.53 R_s has large optical depth ($\tau > 1$) according to radio science and UV occultation measurements (Esposito et al, 1983; Tyler et al., 1983), these charged grains will soon be re-absorbed by the ring particles. When the charge-to-mass ratio is reduced by a factor of 10 and more, all particles will be kept in oscillatory motion (see Fig. 1b and c)

Fig. 2 are for positively charged grains emitted in the same (upward) direction. The group with $q/m \sim 10^{-5}$ e/amu is divided into two components (see Fig. 2a). The population with launching sites inside the synchronous radius (1.866 R_s) – where the velocity of the Keplerian orbit is the same as the corotation velocity – will all move away from the ring plane with their trajectories ending at the planetary surface. The other population of charged grains will be ejected outward becoming interplanetary dust particles. When the charge-to-mass ratio is reduced to 10^{-6} e/amu (see Fig. 2 b), the particle motion will be confined to equatorial region even though the bifurcation of the orbits into inward and outward trajectories is still evident. If $q/m > 10^{-7}$ e/amu, electromagnetic force is much less than the gravitational force, the motion of the charged particles will be mainly Keplerian orbits accompanied by oscillation in the vertical direction. In this case, except for those created in the C ring, the dust particles emitted in the A and B rings will quickly be re-aborbed as they move across the optically thick ring plane.

Fig. 3 and 4 are trajectories of the same sets of charged particles with an initial velocity of 1.5 km s^{-1} but in the downward direction. The patterns of the corresponding orbital dynamics are basically the mirror images of their counterparts with v_z in the upward direction.

If we now consider the dynamics of the charged nano-grains according to the sign of their surface electrostatic potential (ϕ), the positively charged grains with q/m between 10^{-5} and 10^{-6} e/amu and launch sites within the synchronous orbit will be injected into the hemisphere in the same direction of the initial ejection velocity, namely, northern hemisphere for $v_z > 0$, and southern hemisphere for $v_z < 0$.

On the other hand, for negatively charged grains, they tend to follow the effect first pointed out by Northrop and Hill (1983) that only those launched inside the planetocentric distance of 1.53 R_s from the planetary center will reach the southern hemisphere; those ejected at larger radial distances will remain in oscillatory motion above and below the ring plane (see Fig. 1a and 3a). Because the C-ring inside the Northrop-Hill instability limit contains very little mass, it is expected that the corresponding mass

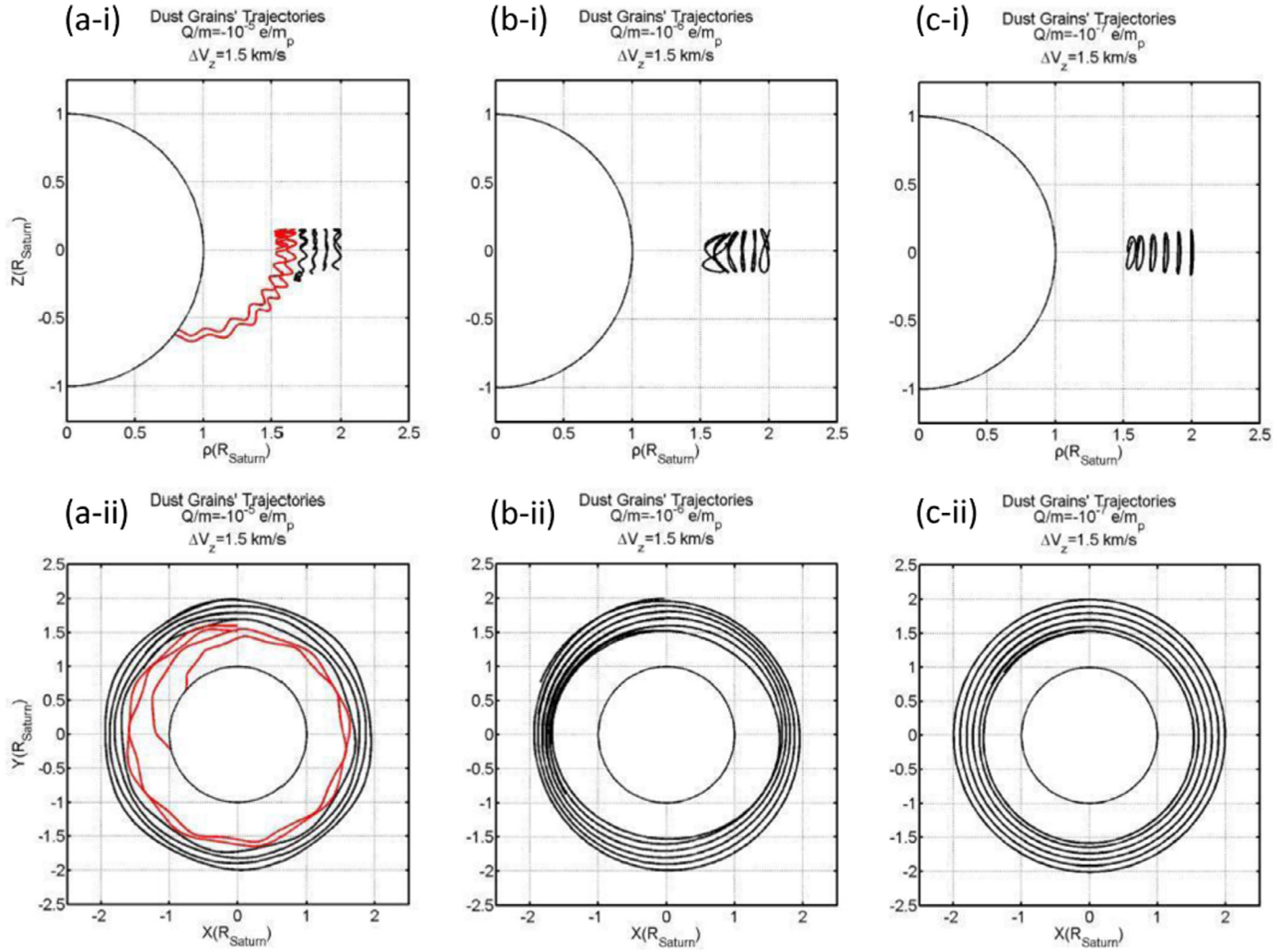

Fig. 1. Trajectories of negatively charged nano-grains ejected initially in upward direction at 1.5 km s^{-1}. Panels (a-i, b-i and c-i) are projections in the ϱ-z plane projection are for three different charge-to-mass ratios: q/m= 10^{-5}, 10^{-6} and 10^{-7}, respectively. Panels (a-ii, b-ii and c-ii) below are trajectories shown in the *x*-*y* plane of the stationary frame of Saturn. The red curves denote trajectories intercepting the planetary surface and the black curves are for particle trajectories in oscillatory motion above and below the ring plane. (For interpretation of the references to color in this figure legend, the reader is referred to the web version of this article.).

injection rate of negatively charged grains would be much smaller than that of the positively charged grains which can be launched directly between the inner edge of the B-ring and the synchronous orbit (see Fig. 2a –b and Fig. 4a–b).

As shown in Figs. 2 and 4, the positively charged nano-grains have another interesting property. That is, they could be launched into low-inclination orbits either intercepting Saturn's surface or spiraling outward (Fig. 2b–i and Fig. 4b–i). This means that the Cassini spacecraft might detect a flux of tiny ring dust emitted from the main rings when it crosses the ring plane outside the F ring.

The same calculations have been repeated for the case of ejection speed $V_z = 2.5$ km s^{-1}. Similar dynamical behaviors as for $V_z = 1.5$ km s^{-1} are observed.

The outward motion of the positively charged nano-grains with q/m $\sim 10^{-5}$ – 10^{-6} when ejected outside the synchronous orbit can be explained in the following. That is, the gyro-radii of these grains are large enough that their motion can no longer be described in terms of the guarding center approximation. On the other hand, they are still significantly affected by the Lorentz force. The particle motions with q/m = 10^{-6} shown in Fig. 2.b and 4-b are good examples. Following the analysis given by Horanyi et al. (1993) in the case of the ejection of high-speed nano-grains from the orbital region of the Io plasma torus in the Jovian system, we can first use the formula of $E = V_c \times B = (r \times \Omega) \times B$ where Ω ($=1.707 \times 10^{-4}$ rad s^{-1}) is the angular speed of Saturn's rotation to derive the corotational electric field to be $E = 0.216\ (R_s/r)^2$ V/m. Note that we have used the dipole approximation, $B = B_0(R_s/r)^3$, to compute the equatorial magnetic field at radial distance r. From $q = 700\ a_\mu \Phi_v\ e$, $q/m = 1.7 \times 10^{-9}/a_\mu{}^2\ (\Phi_v/6)\ e/m_p$. The electrostatic force due to the outward-pointing corotational electric field is then $F_c = 0.087\ \Phi_v a_\mu / r^2$. Newton. Finally, the ratio of the electrostatic force and the gravitational force is simply $\lambda = 5.5 \times 10^{-4}\ \Phi_v\ / a_\mu{}^2$. Thus, for $a_\mu \sim 0.057\ \mu$m (or 57 nm), $\Phi = 6$ V (at q/m = 3.6×10^{-7} e/m_p), and $\lambda \sim 1$, namely, the electrostatic force is as strong as the gravitational pull. The consequence is that the positively charged grains outside the synchronous radius will gain energy and be accelerated away from the planet by the corotational electric field. On the other hand, those produced inside the synchronous orbit will have the inward electrostatic force adding to the gravitational force and be attracted towards the planetary surface. For larger particles with q/m $\sim 10^{-7}$ (see Fig. 2c for example) $\lambda \sim 0.2$ and the positively charged particles will be trapped in Keplerian motion albeit with vertical oscillation of finite amplitude. For smaller grains with q/m = 10^{-5} (see Fig. 2-a for example), the interplay between the gyromotion and enhanced inward force would lead to field

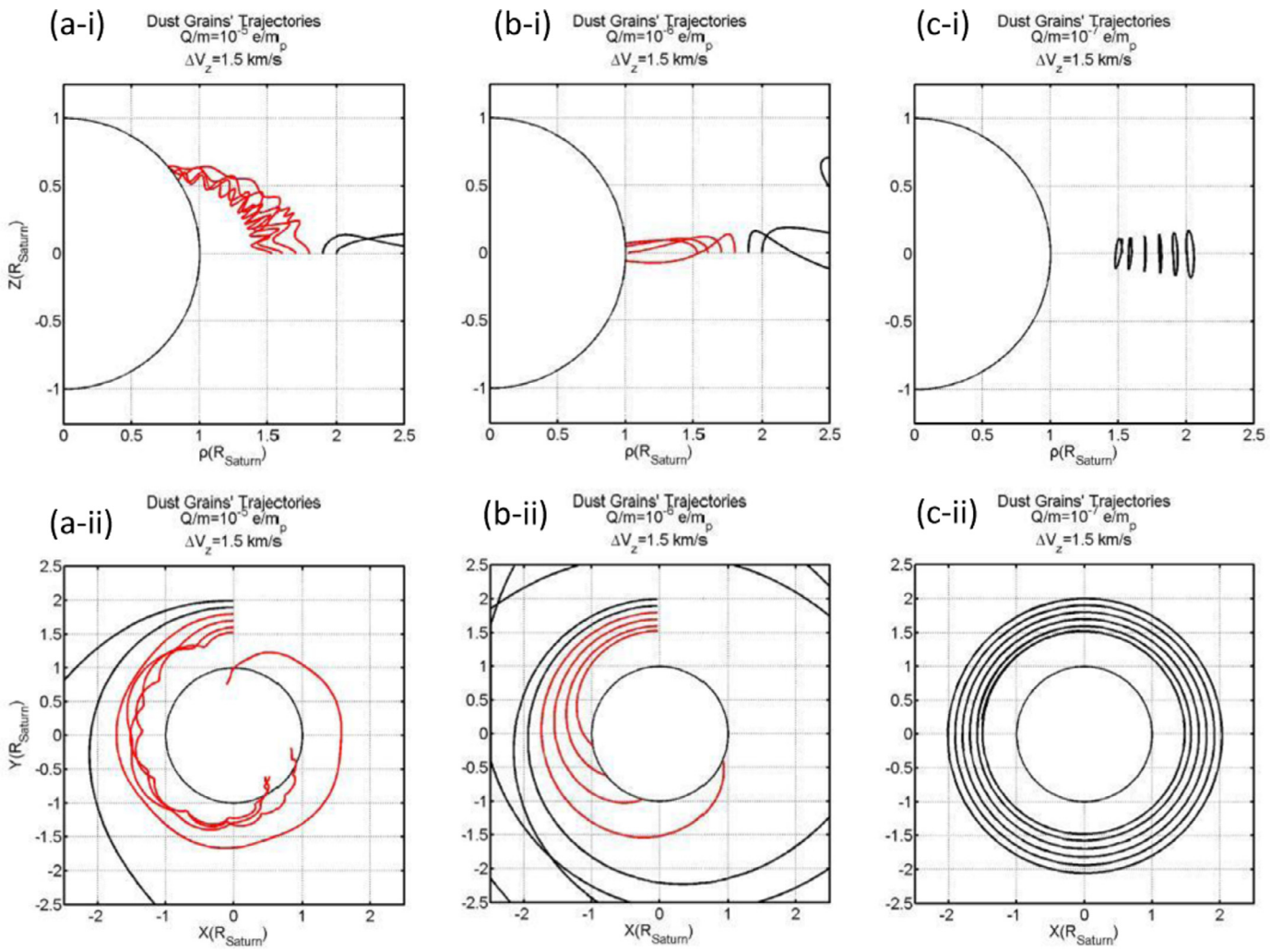

Fig. 2. Same as Fig. 1 with $v_z = 1.5$ km s^{-1} but for positively charged nano-grains ejected initially in upward direction.

aligned trajectories of the grains injected inside the synchrotron orbit but spiraling outward outside of this critical distance.

4. Discussion and summary

The plasma environment of the Saturnian rings is not well known. The plasma content could be significantly depleted because of the ring absorption effect (Tokar et al., 2005; Waite et al., 2005). In this event, the dust grains are expected to be positively charged on the sunlit side of the ring plane (Ip, 1984b). On the other hand, the photo-sputtering of the icy ring particles could lead to the formation of a layer of ring atmosphere of mainly oxygen molecules and oxygen ions (Johnson and Quickenden, 1997; Johnson et al., 2006; Bouhram et al., 2006; Luhmann et al., 2006; Tseng et al., 2010). The interaction process among the ring plasma, ring particles and the small dust grains is still to be investigated. As a follow-up to the study of Liu and Ip (2014) on the trajectories of negatively and positively charged nano-grains launched from circular Keplerian orbits, we have examined tiny charged grains produced in micrometeoroid/meteoroid impacts on the ring particles. The basic assumption of our parametric calculations is that a continuous flux of nano-grains will be generated in the impact plumes and they move mostly in the vertical directions once leaving the ring plane of large optical depth. In this simplified picture, it is further assumed that the nano-grains with an initial speed between 1.5 and 2.5 km s^{-1} will be electrostatically charged by photoemission and plasma charging.

Our numerical results can in principle be applied to both negatively and positively charged nano-grains. It is noted that positively charged grains have the peculiar behavior that their injection pattern is dictated by which direction they are first ejected (see Figs. 2 and 4). On the other hand, negatively charged grains always fall into the southern hemisphere at latitude magnetically connected to the ring plane within the Northrop-Hill limit of 1.53 R_s (see Figs. 1 and 3).

In brief, it is found that the nano-grains created in the main rings within the synchronous radius could be injected into both hemispheres of the Saturnian atmosphere if they are positively charged to a certain range of q/m ratio ($\sim 10^{-5}$ – 10^{-6} e/amu). The water transport pattern of the negatively charged nano-grains is asymmetrical as only the southern hemisphere will be subjected to the influx. In comparison to the positively charged nano-grains, the mass influx of negatively charged nano-grains could be smaller than that of their positively charged counterparts because the corresponding source region is located within the C ring which is much reduced in mass content.

One interesting atmospheric phenomenon of the Saturnian atmosphere has to do with the observed occurrence of the Great White Spots (GWS) and giant storms between 5° and 60° northern latitude in nearly every 30 years since 1876 (Sanchez-Lavega and Battanar, 1987; Fischer et al., 2013). Li and Ingersoll (2015)

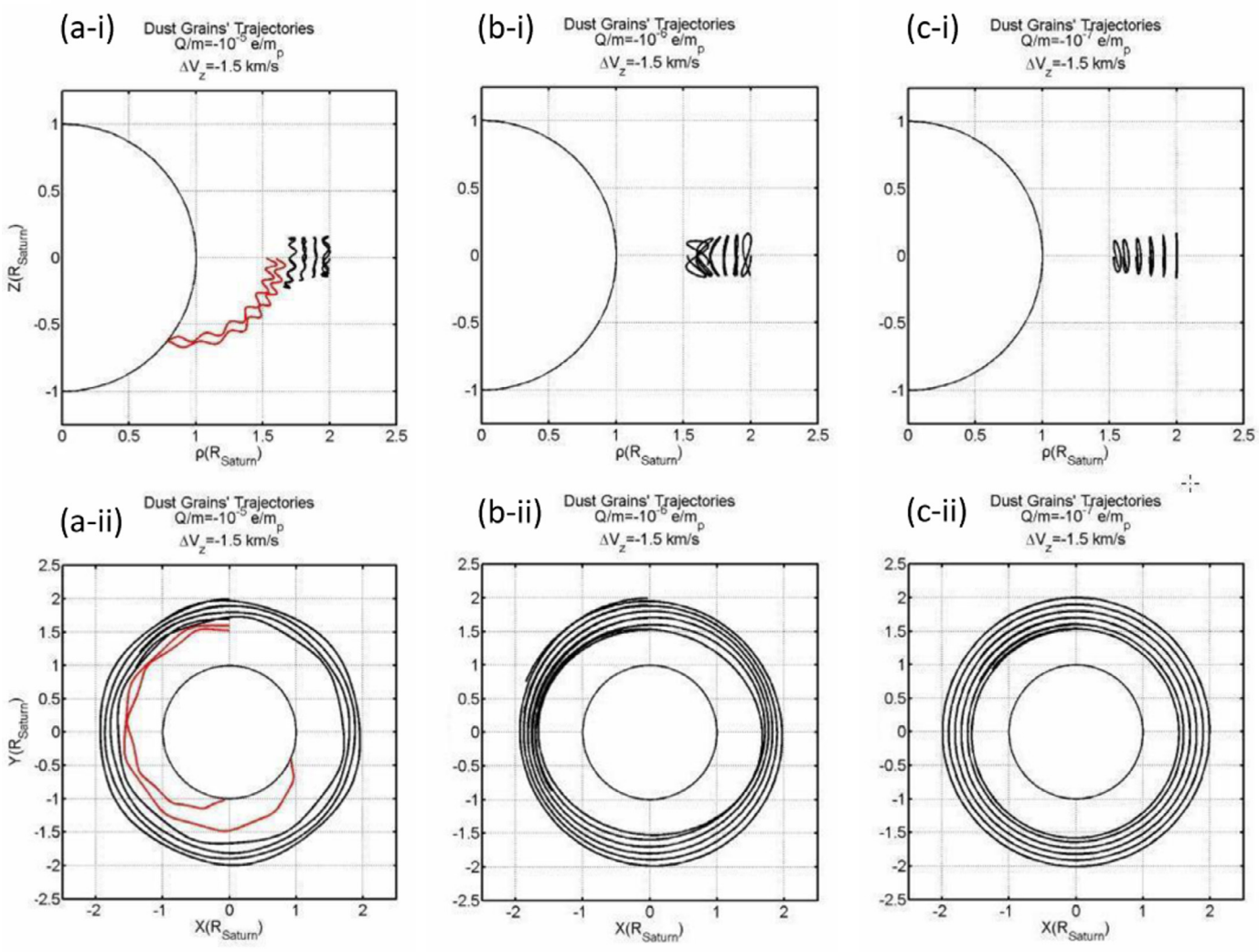

Fig. 3. Same as Fig. 1 with $v_z = -1.5\ \mathrm{km\ s^{-1}}$ but for negatively charged nano-grains ejected initially in downward direction.

explained the quasi-periodic formation of the planet-circling storms in terms of a water-loading mechanism in Saturn's troposphere. Except for the asymmetric injection of negatively charged nano-grains into the southern hemisphere which might suppress the GWS-generating atmospheric instability, there is no obvious relation to the top-down scenario of mass transfer from the ring system to Saturn's upper atmosphere.

Our present study of the trajectories of charged nano-grains might have some other interesting implications. That is, in a recent observational study of the H_3^+ infrared emission at Saturn, an interesting correlation of the H_3^+ brightness and the ring structure was found (O'Donoghue et al., 2013). That is, atmospheric regions of weaker H_3^+ emission tend to be magnetically connected to the B and C rings while stronger emission was found in the vicinity of the latitudes connected to the ring gaps. Such a ring rain effect, however, is not consistent with the picture of "direct injection" of ions or charged dust grains – from circular or near-circular Keplerian orbits – which pattern of precipitation should have very strong hemispherical asymmetry and be essentially confined within the synchronous radius of 1.87 R_S see also (Bouhram et al., 2006; Luhmann et al., 2006; Tseng et al., 2010; Liu and Ip, 2014).

A possible solution to this dilemma might come from borrowing the observational result of enhanced H_3^+ emission at the footpoint of the flux tube of Io near the Jovian auroral zone (Connerney et al., 1993). In other words, the latitudinal variability of the H_3^+ brightness across Saturn could be caused by enhanced production instead of quenching. This may be achieved by the establishment of field-aligned current systems connecting the rings to the ionosphere analogous to the electrical current system generated by the gas and dust cloud emitted from Enceladus (Sakai et al., 2013; Farrell et al., 2014).

In the present scenario, the dust clouds would be the product of interplanetary meteoroid bombardment of the Saturn rings. If the context of the spoke formation, Morfill et al. (1983) estimated that the ring mass erosion rate due to micrometeoroid impact could reach a value of $\dot{M}_E \sim (0.8\text{–}7) \times 10^9\ \mathrm{g\ s^{-1}}$. And the corresponding mass production rate of impact water vapor would be $\dot{M}_V \sim (0.75\text{–}6) \times 10^6\ \mathrm{g\ s^{-1}}$. If the lower limits are used, the nano-grains created from recondensation of the expanding vapor clouds could have a mass production rate of approximately $3 \times 10^5\ \mathrm{g\ s^{-1}}$ at maximum. Following the initial formulation of the pickup current balancing the $J \times B$ Lorentz force with the momentum change required to accelerate the new-born nano-dust to full corotation motion (Ip and Axford, 1980; Goertz, 1980), the total pickup current $I \sim \dot{M}_V\ \Delta V/BL$ where ΔV is the difference between the corotation speed and the Keplerian velocity, and L is the length scale of the pickup region. With $\Delta V \sim 2\ \mathrm{km\ s^{-1}}$, $L \sim 0.5\ R_s$, and $B \sim 3.1 \times 10^{-3}$ G, we have I ~ 32 KA in total. This current is much smaller than the estimate of 6.6×10^5 A for Ganymede's field-aligned current (Ip and Kopp, 2002) that generates a pair of ultraviolet hot spots near

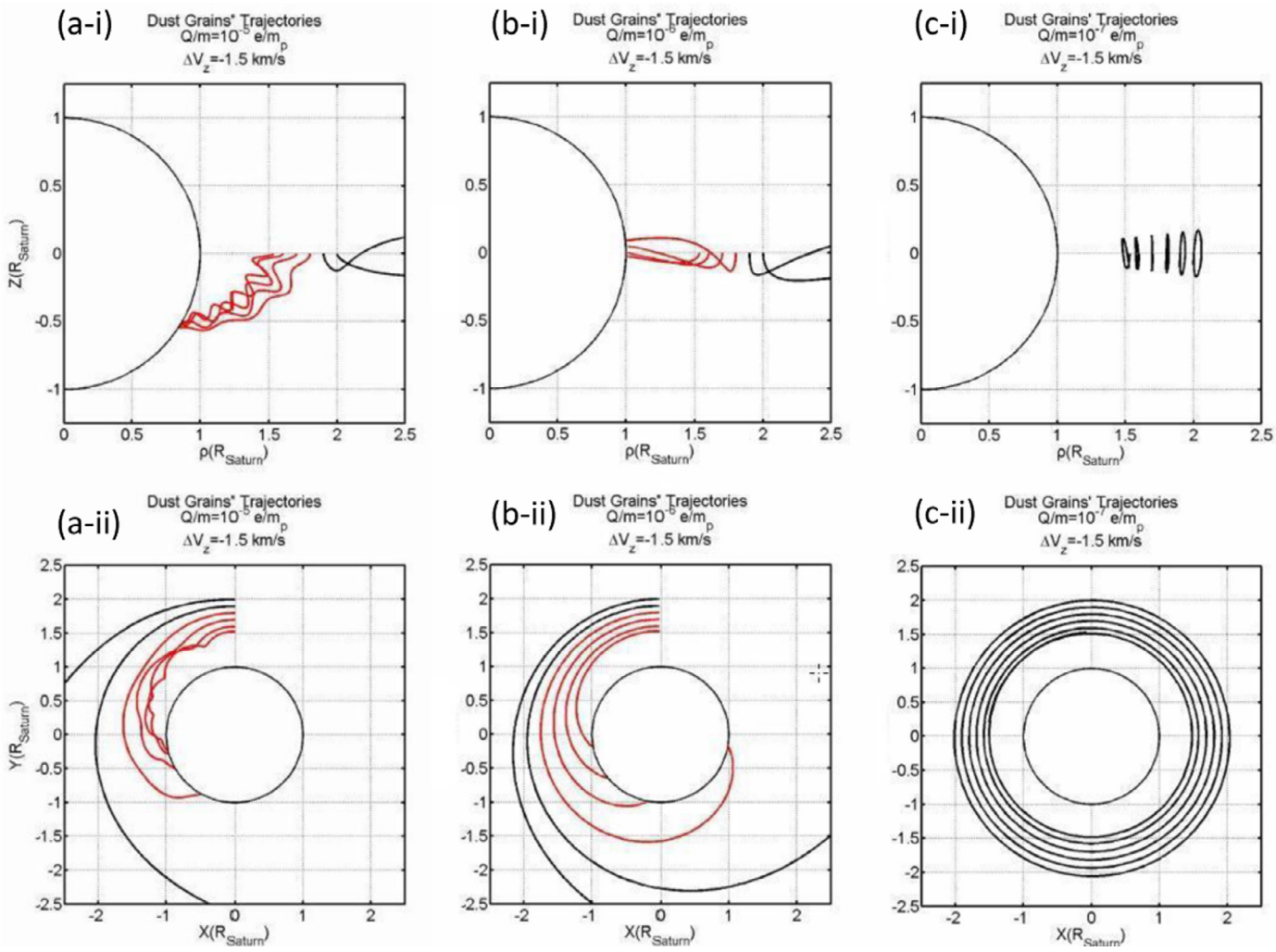

Fig. 4. Same as Fig. 1 with $v_z = -1.5\ km\ s^{-1}$ but for positively charged nano-grains ejected initially in downward direction.

the Jovian auroral oval (Clarke et al., 2002). However, if channeled in thin current sheets near the boundaries of the ring gap or other regions, some additional ionization effect could possibly be generated and enhancement of H_3^+ might be expected at the latitudes magnetically connected to the Cassini Division and other ring gaps. This effect plus the orbital pattern of the positively charged nano-grains could be related to the intriguing measurements by the Cassini radio science experiment that Saturn's ionospheric density increases with latitude (Kliore et al., 2014).

It is also noted that the Northrop-Hill instability of vertical motion of the negatively charged nano-grains leads to the boundary of the B and C rings (Northrop and Hill, 1982, 1983). The continuous mass loss process via the ejection of small grains at radial distance inside 1.53 R_S could have important effect on the estimation of the time scale related to ballistic transport (Ip, 1984c; Cuzzi and Estrada, 1998). That is, the siphoning of the charged nano-grains at this critical radius by electromagnetic force could be effective in sharpening the discontinuity in the mass distribution across the B and C ring boundary in tandem with the ballistic transport mechanism. Besides, the radial component is also noteworthy in mass transport across the ring system. In the extreme situation, positively charged tiny dust could be ejected into escaping orbits away from Saturn (cf. Horanyi et al., 1993). Their presence might therefore be detected by the Cassini spacecraft during ring plane crossing outside the F ring orbit. For one thing, if taking into account the fact that the relative impact speed between the spacecraft and the ring dust will reach about $30\ km\ s^{-1}$, the antenna of the Radio and Plasma Wave Science (RPWS) experiment might be able to register the electromagnetic signals generated by impacts of micron to sub-micron icy grains (see Aubier et al., 1983; Kurth et al., 2006).

From the above description, it is expected that the Proximal mission in 2016-2017 of the Cassini-Huygens Mission will bring a wealth of information clarifying the role of injection of nano-grains or ions in shaping the Saturnian ionosphere and that of the ring rain effect on the H_3^+ emission at the mid-latitude atmosphere. Furthermore, it would be interesting to search for field-aligned currents which could result from dust-plasma interaction in the rings.

Acknowledgment

We thank the Reviewer for useful comments and suggestions. This work is partially supported by MOST 104-2119-M-008-024 (TANGO II) and MOST 104-2111-M-008-020 (Space) and MOE under the Aim for Top University program NCU, and Macau Technical Fund: 017/2014/A1 and 039/2013/A2.

References

Aubier, M.G., Meyer-Vernet, M., Pedersen, B.M., 1983. Shot noise from grain and particle impacts in Saturn's ring plane. Geophys. Res. Lett. 10, 5–8.
Bouhram, M., Johnson, R.E., Berthelier, J.-J., et al., 2006. A test-particle model of the atmosphere/ionosphere system of Saturn's main rings. GeoRL 33, 33–36 L05916.

Clarke, J.T., Ajello, J., Balleter, G., et al., 2002. Ultraviolet emissions from the magnetic footprints of Io, Ganymede and Europa on Jupiter. Nature 415, 997–1000.
Charnoz, S., Salmon, J., Crida, A., 2010. The recent formation of Saturn's moonlets from viscous spreading of the main rings. Nature 465, 752–754.
Collette, A., Drake, K., Mocker, A., et al., 2013. Time-resolved temperature measurements in hypervelocity dust impact. Planet. Space. Sci. 89, 58–62.
Connerney, J.E.P., Baron, R., Satoh, T., et al., 1993. Images of excited H3+ at the foot of the Io flux tube in Jupiter's atmosphere. Science 262, 1035–1038.
Connerney, J.E.P., Waite, J.H., 1984. New model of Saturn's ionosphere with an influx of water from the rings. Nature 312, 136–138.
Connerney, J.E.P., Ness, N.F., Acuna, M.H., 1982. Zonal harmonic model of Saturn's magnetic field from Voyager 1 and 2 observations. Nature 298, 44–46.
Cuzzi, J.N., Estrada, P.R., 1998. Compositional evolution of Saturn's rings due to meteoroid bombardment. Icar 132, 1–35.
Eichhorn, G., 1976. Analysis of the hypervelocity impact process from impact flash measurements. Planet. Space Sci. 24, 771–781.
Esposito, L.W., Callaghan, M., Simmons, K.E., et al., 1983. Voyager photopolarimeter stellar occultation of Saturn's rings. JGR 88, 8643–8649.
Farrell, W.M., Wahlund, J.-E., Morooka, M., et al., 2014. An estimate of the dust pickup current at Enceladus. Icarus 239, 217–221.
Fischer, G., Kurth, W.S., Gurnett, D.A., et al., 2013. A giant thunderstorm on Saturn. Natur 475, 75–77.
Goertz, C.-K., 1980. Io's interaction with the plasma torus. J. Geophys. Res. 85, 2949–2956.
Horanyi, M., Morfill, G., Gruen, E., 1993. Mechanism for the acceleration and ejection of dust grains from Jupiter's magnetosphere. Nature 363, 144–146.
Hyodo, R., Ohtsuki, K., 2014. Collision disruption of gravitational aggregates in the tidal environment. ApJ 787, 1–14.
Ip, W.-H., 1983. On plasma transport in the vicinity of the rings of Saturn: a siphon flow mechanism. JGR 88, 819–822.
Ip, W.-H., 1984a. On the equatorial confinement of thermal plasma generated in the vicinity of the rings of Saturn. JGR 89, 395–398.
Ip, W.-H., 1984b. Electrostatic charging of the rings of Saturn: a parameter. JGR 89, 3829–3836.
Ip, W.-H., 1984c. Ring torque of Saturn from interplantary meteoroid impact. Icar 60, 547–552.
Ip, W.-H., 1995. The exospheric systems of Saturn's rings. Icar 115, 295–303.
Ip, W.-H., Axford, W.I., 1980. A weak interaction model for Io and the jovian magnetosphere. Nature 283, 180–183.
Ip, W.-H., Kopp, A., 2002. Resistive MHD simulations of Ganymede's magnetosphere 2. Birkeland currents and particle energetics. J. Geophys. Res. 107 (A12), 1491–1497.
Jurac, S., Richardson, J.D., 2005. A self-consistent model of plasma and neutrals at Saturn: neutral cloud morphology. JGR 110, A09220. doi:10.1029/2004JA010635.
Jurac, S., Richardson, J.D., 2007. Neutral cloud interaction with Saturn's main rings. GeoRL 34, L08102. doi:10.1029/2007GL029567.
Johnson, R.E., Quickenden, T.I., 1997. Photolysis and radiolysis of water ice on outer solar system bodies. JGR 102, 10985. doi:10.1029/97JE00068.
Johnson, R.E., Luhmann, G.G., Tokar, R.L., et al., 2006. Production, ionization and redistribution of Saturn O2 ring atmosphere. Icar 180, 393–402.
Kliore, A.J., Nagy, A., Asmar, S., et al., 2014. The ionosphere of Saturn as observed by the Cassini Radio Science System. Geophys. Res. Lett. doi:10.1002/2014GL060512.
Kurth, W.S., Averkamp, T.F., Gurnett, D.A., et al., 2006. Cassini RPWS observations of dust in Saturn's E ring. Planet. Space Sci. 54, 988–998.
Li, C., Ingersoll, A.P., 2015. Moist convection in hydrogen atmospheres and the frequency of Saturn's giant storms. Natur-Geo 8, 398–401.
Liu, C.M., Ip, W.-H., 2014. A new pathway of Saturnian ring-ionosphere coupling via chrged nanograins. ApJ 786, 34. doi:10.1088/0004-637X/786/1/34.
Luhmann, J.G., Johnson, R.E., Tokar, R.L., et al., 2006. A model of the ionosphere of Saturn's rings and its implications. Icar 181, 465–474.
Moore, L., Mendillo, M., 2007. Are plasma depletions in Saturn's ionosphere a signature of time-dependent water input? GeoRL 34, L12202. doi:10.1029/2007GL029381.
Moore, L., Nagy, A.F., Kliore, A.J., et al., 2006. Cassini radio occultations of Saturn's ionosphere: model comparisons using a constant water flux. GeoRL 33, L22202. doi:10.1029/2006GL027375.
Morfill, G.E., Fechtig, H., Gruen, E., et al., 1983. Some consequences of meteoroid impacts on Saturn's rings. Icar 55, 439–447.
Moses, J.I., Bass, S.F., 2000. The effects of external material on the chemistry and structure of Saturn's ionosphere. JGR 105, 7013–7052.
Murray, C.D., Cooper, N.J., Williams, G.A., et al., 2014. The discovery and dynamical evolution of an object at the outer edge of Saturn's A ring. Icar 236, 165–168.
Northrop, T.G., Connerney, J.E.P., 1987. A micrometeorite erosion model and the age of Saturn's rings. Icar 70, 124–137.
Northrop, T.G., Hill, J.R., 1982. Stability of negatively charged dust grains in Saturn's ring plane. JGR 87, 6045–6051.
Northrop, T.G., Hill, J.R., 1983. The inner edge of Saturn's B ring. JGR 88, 6102–6108.
O'Donoghue, J., Stallard, T.S., Melin, H., et al., 2013. The domination of Saturn's low-latitude ionosphere by ring "rain". Natur 496, 193–195.
Ohtsuki, K., 1993. Capture probability of colliding planetesimals - Dynamical constraints on accretion of planets, satellites, and ring particles. Icar 106, 228–246.
Sakai, S., Watanable, S., Morooka, M.W., et al., 2013. Dust-plasma interaction through magnetosphere-ionosphere coupling in Saturn's plasma disk. Planet. Space Sci. 75, 11–16.
Sanchez-Lavega, A., Battaner, E., 1987. The nature of Saturn's atmospheric Great White Spots. Astron. Astrophys. 185, 315–326.
Tiscareno, M.S., Mitchell, C.J., Murray, C.D., et al., 2013a. Observations of ejecta clouds produced by impacts onto Saturn's rings. Science 340, 460–464.
Tiscareno, M.S., Hedman, M.M., Burns, J.A., et al., 2013b. Compositions and origins of outer planet systems: Insights from the Roche critical density. APJL 765, L28.
Tokar, R.L., Johnson, R.E., Thomsen, M.F., et al., 2005. Cassini observations of the thermal plasma in the vicinity of Saturn's main rings and the F and G rings. Geophys. Res. Lett. 32, L14S04. doi:10.1029/2005GL022690.
Tyler, G.L., Marouf, E.A., Simpson, R.A., et al., 1983. The microwave opacity of Saturn's rings at wavelengths of 3.6 and 13 cm from Voyager 1 radio occultation. Icar 54, 160–188.
Tseng, W.L., Ip, W.-H., Johnson, R.E., et al., 2010. The structure and time variability of the ring atmosphere and ionosphere. Icar 206, 382–389.
Waite, J.H., Cravens, T.E., Ip, W.-H., et al., 2005. Oxygen ions observed near Saturn's A ring. Science 307, 1260–1262.